Complement C5a receptor facilitates cancer metastasis by altering T cell responses in the metastatic niche

Surya Kumari Vadrevu[a,*], Navin K. Chintala[a,*], Sharad K. Sharma[a,*], Priya Sharma[a], Clayton Cleveland[a], Linley Riediger[a], Sasikanth Manne[a], David P. Fairlie[b], Wojciech Gorczyca[c], Othon Almanza[d], Magdalena Karbowniczek[a] and Maciej M. Markiewski[a]

[a]Department of Immunotherapeutics and Biotechnology, School of Pharmacy, Texas Tech University Health Science Center, 1718 Pine Street, Abilene, Texas, 79601, USA

[b]Division of Chemistry and Structural Biology, Institute for Molecular Bioscience, University of Queensland, 306 Carmody Rd. Brisbane, Queensland, 4072, Australia

[c]Bioreference Laboratories, Elmwood Park, New Jersey and Regional Cancer Care Associates, Hackensack, 100 First Street, New Jersey, 07601, USA

[d]Clinical Pathology Associates, 1150 N 18th Street, Abilene, Texas, 79601, USA

[*]These authors contributed equally to this work.

Corresponding author: Maciej M. Markiewski

1718 Pine Street, Abilene, TX 79601

Phone: 325-696-0430

E-mail: maciej.markiewski@ttuhsc.edu

Conflict of interest statement:

MMM has a patent application for use of complement inhibition in anticancer therapy.

Running title: Role of C5a receptor in breast cancer metastasis.

Key words: Complement, C5a, metastasis, premetastatic niche, T cells.

Abstract

The impact of complement on cancer metastasis has not been well studied. In this report, we demonstrate in a preclinical mouse model of breast cancer that the complement anaphylatoxin C5a receptor (C5aR) facilitates metastasis by suppressing effector $CD8^+$ and $CD4^+$ T cell responses in the lungs. Mechanisms of this suppression involve recruitment of immature myeloid cells to the lungs and regulation of TGF-β and IL-10 production in these cells. TGF-β and IL-10 favored generation of T regulatory cells (T_{reg}) and Th2 oriented responses that rendered $CD8^+$ T cells dysfunctional. Importantly, pharmacological blockade of C5aR or its genetic ablation in C5aR-deficient mice were sufficient to reduce lung metastases. Depletion of $CD8^+$ T cells abolished this beneficial effect, suggesting that $CD8^+$ T cells were responsible for the effects of C5aR inhibition. In contrast to previous findings, we observed that C5aR signaling promoted T_{reg} generation and suppressed T cell responses in organs where metastases arose. Overall, our findings indicated that the immunomodulatory functions of C5aR are highly context dependent. Furthermore, they offered proof-of-concept for complement-based immunotherapies to prevent or reduce cancer metastasis.

Introduction

Preventing cancer metastasis is a Holy Grail of cancer therapy, as the majority of cancer deaths are attributed to this process (1). However, progress in this area has been limited by our poor understanding of its mechanism. Recent evidence has indicated that, in addition to the mechanisms operating in neoplastic cells (2), alterations in host homeostasis, particularly in the immune system, contribute to metastasis (3). These alterations occur in the primary tumor microenvironment (2), however roles for

host-derived cells and mediators at sites distal to the tumor have also been reported (4). An important concept in tumor metastasis is the formation of premetastatic niches, in which malignant tumors prepare the environment of remote organs to receive metastatic cells by altering host homeostasis in these organs prior to tumor cell arrival. Since these changes precede metastases, therapeutic targeting of these premetastatic niches might prevent metastasis. The existence of premetastatic niches was proposed over a hundred years ago (3), but only recently have components of these niches been identified and they include myeloid-derived suppressor cells (MDSCs) (5-8). The primary tumor hypoxia inducible factors (9), serum amyloid A3 induced by S100A8 and A100A9 (10), and S1PR1-STAT3 signaling (11) have been suggested to be involved in recruiting these cells from the bone marrow to premetastatic organs. However, mechanisms governing recruitment of various cells to premetastatic organs and how the cells facilitate metastases are not clear. It is conceivable that MDSCs, which suppress anti-tumor T cell responses in primary tumors and peripheral lymphoid organs (12), shield metastasizing tumor cells from immune attack at distant sites targeted by metastases (5). However, in contrast to primary sites, the significance of T cell suppression in premetastatic niches remains unclear (13). Since the complement anaphylatoxin C5a, a potent chemoattractant in inflammatory reactions (14), activates and attracts immunosuppressive cells to primary tumors (15), we hypothesize that C5a also contributes to immunosuppression facilitating metastases in distant sites.

Using a mouse model of breast cancer (16), we show that C5a receptor 1 (C5aR) contributes to metastasis by suppressing T cell responses in the lungs, since reduction in metastatic burden in the lungs by C5aR-inhibition was abolished by $CD8^+$ T cell

depletion. C5aR blockade resulted in increased recruitment of $CD4^+$ and $CD8^+$ T cells and induction of Th1/Tc1-biased T cell responses. Mechanisms of C5aR-mediated immunosuppression involved recruitment of MDSCs and generation of T_{reg} cells and regulating production of the immunosuppressive cytokines, TGF-β and IL-10, in myeloid cells. Relevance of our findings for human breast cancer was underscored by identifying MDSCs and complement deposition in tumor draining lymph nodes (TDLNs) of breast cancer patients.

Materials and Methods

Mice and cell lines

Balb/c wild-type (WT) and C5aR-deficient ($C5aR^{-/-}$) mice were from The Jackson Laboratory. $C5aR^{-/-}$ mice were backcrossed ten generations to Balb/c before being made homozygous. Upon arrival to The Jackson Laboratory, these mice were bred at least one generation to Balb/c. Mice were housed in the animal facility of Texas Tech University Health Sciences Center (TTUHSC). Water and standard rodent diet were provided *ad libitum*. All experiments were approved by the Committee of Institutional Animal Care and Use according to the guidelines of the National Institutes of Health. 4T1 (CRL-2539, ATCC) and 4T1-luc2-GFP (128090, Caliper/PerkinElmer) tumor cell lines were maintained in cell culture media as recommended by suppliers and routinely tested for the absence of mycoplasma (Aldevron, ND, USA). The information of tumor model development and $CD8^+$ T cell depletion is provided in supplemental materials.

Complement C5a receptor antagonism

A selective antagonist of C5aR, the cyclic peptide Ac-(cyclo-2,6)-F[OP(D-Cha)WR] was used for C5aR-blockade. This compound, originally named 3D53 and also licensed as PMX53 (17) but abbreviated as C5aRA herein, specifically binds to C5aR1 and does not bind to the second C5a receptor (C5L2) or to the C3a receptor (18). It was synthesized and characterized as described (19), dissolved in sterile PBS, and injected s.c. at a dose of 1 mg/kg body weight, every 2–3 days beginning on day 7 after tumor cell injection (3.3 μmol/kg body weight per week) (15); or day 12-15 after 4T1-luc2-GFP cell injection when palpable breast tumors (approximately 5 mm in diameter) were observed. The delay in administering C5aRA when 4T1-luc2-GFP cells were injected in mice was due to the slower tumor growth compared to the parent 4T1 cell line. Control mice received sterile PBS.

Tissue and cell processing, immunofluorescence/immunohistochemistry, quantitative PCR, ELISA for complement fragments, and bronchoalveolar lavage isolation

Mouse organs were fixed in 10% (v/V) formalin, 4% paraformaldehyde or froze in optimum cutting temperature (O.C.T) medium. Formalin fixed samples were routinely processed for histology and immunohistochemistry. Paraformaldehyde-fixed lungs were immersed in 30% sucrose, washed in PBS, and then froze in O.C.T. medium. Frozen samples were sectioned with cryostat (Leica) for immunofluorescence or quantification of GFP^+ metastases. Blood samples after erythrocyte lysis with ACK buffer (118-156-101, Quality Biological), were stained for FACS. Lungs were digested in the digestion

buffer (collagenase D) and mechanically disintegrated and passed through 40 µm cell strainers (BD Biosciences) to obtain single-cell suspensions. Spleens were mechanically disintegrated and passed through cell strainers. Formalin fixed sections were stained with hematoxylin & eosin (H&E) to quantify metastases by digital pathology algorithms. Details of immunofluorescence/immunohistochemistry procedures, information on scoring metastases, quantitative PCR, C5a and C3 ELISA, Bronchoalveolar lavage (BAL) isolation, are provided in supplemental materials.

Antibodies, functional assays, and FACS

For T cell stimulation assays, cells were incubated in the presence of brefeldin-A and monensin (BD Biosciences) in CD3 and CD28 antibodies adsorbed 96-well plates (17A2 and 37.51, eBioscience) for 6 to 8 h. Cytokine production was assessed by intracellular cytokine staining. For analysis of C5aR expression, cells were incubated with rabbit polyclonal anti–mouse C5aR (C1150-32; BD Biosciences) or rabbit isotype-matched control antibody (550875; BD Pharmingen) and then with FITC–conjugated anti-rabbit IgG (F0112; R&D Systems). In addition, rat mAb to mouse C5aR (20/70; Hycult Biotechnology) or rat isotype-matched control antibody (553928; BD Pharmingen), followed by FITC–conjugated anti–rat IgG (81–9511; Zymed-Invitrogen) were used.

To study the impact of C5aR-signaling in MDSCs on the polarization of T cell responses, groups of tumor-bearing Balb/c WT mice were injected with C5aRA or PBS as described in supplemental materials. On day 30, mouse lungs were harvested for MDSCs isolation, which was performed with MDSC isolation kit (miltenyi). Naïve $CD4^+$ T

cells were negatively sorted (miltenyi) from splenocytes of non-tumor-bearing mice. Purity of cells was verified by FACS staining and found to be >98%. $CD4^+$ T cells and lung-derived MDSCs were co-cultured in 1:5 ratios in a 24-well plate previously coated with CD3/CD28 antibodies. $CD4^+$ T cell cultures were harvested at day 5 and intracellular staining for IFN-γ and IL-4 was performed after stimulation as described in supplemental materials. Additional information on antibodies, staining and gating strategies is also provided in supplemental materials.

Digital image analysis

H&E stained lung and liver sections were scanned and digitalized (Aperio Technologies, Inc.). Quality control of digital whole slide images (WSI) and all further analysis were performed using ImageScope (Aperio). Aperio Genie Classifier was used for analyzing all the WSI.

Statistical analysis

At least five mice per group were included in each experiment, except one experiment with n=3. Data were analyzed with un-paired t-test or non-parametric Mann-Whitney test, depending on results of the normality test (Kolmogorov-Smirnov). For data with the normal distribution two-tailed un-paired t-test (t-test) was used. Two-tailed un-paired t-test with Welch's correction (t-test with Welch's correction) was used for data having significant differences in variances between groups. For data lacking the normal distribution two-tailed non-parametric Mann-Whitney (Mann-Whitney test) test was used. For multiple comparisons One-way ANOVA and for normalized data from qPCR one sample t-test were used. Outliers were identified using Grubb's test at α=0.05. All

statistical analysis was done with Graph Pad Prism 6 software. Statistical significance was based on a value of $P \leq 0.05$. For $P > 0.05$, 95% confidence interval (CI) was used to draw conclusions.

Results

C5aR signaling facilitates lung and liver metastases

C5aR-signaling was found to promote tumor growth by modulating anti-tumor immunity in a syngeneic mouse model of cervical cancer (15). However, its role in metastatic spread of cancer has not been explored. Therefore, we investigated whether C5aR contributes to metastasis. We found that C5aR deficiency reduced lung (Fig. 1A, B) and liver (*Supplemental* Fig. S1A, B) metastatic burden without significantly affecting the growth of primary breast tumors (Fig. 1C) in a syngeneic model of breast cancer (4T1), which closely mimics stage IV of human breast cancer (16). Decreased metastatic burden together with the lack of an impact of C5aR-deficiency on primary tumor growth suggests that C5aR promotes metastasis through mechanisms independent of those operating in primary tumors. In addition, since 4T1 tumor cells do not express C5aR (*Supplemental* Fig. S1C), C5aR-signaling in tumor cells does not directly govern metastasis to distant organs. To support our data from genetically modified mice, we examined the impact of pharmacological inhibition of C5aR on metastases in mice bearing GFP-expressing 4T1 breast tumors (4T1-GFP^+). Metastatic burden was markedly reduced in mice treated with C5aR antagonist (C5aRA) compared to placebo treated control mice (Fig. 1D-F). Importantly, 75% of the mice that received C5aRA remained metastases-free (Fig. 1E), while 25% of the mice developed fewer

and smaller lung metastases than control mice (Fig. 1E, F). Despite this substantial impact on metastasis, similar to observations from the experiments with C5aR knockout mice, pharmacological inhibition of C5aR by C5aRA did not affect growth of the primary tumors in this study (Fig. 1G).

C5aR inhibits the recruitment and function of $CD4^+$ and $CD8^+$ T cells in the lungs and livers of breast tumor-bearing mice

Anti-tumor $CD4^+$ and $CD8^+$ T cells are considered to be major effectors that limit tumor growth at primary sites and our previous study linked C5aR to anti-tumor T cell responses (15). However, no role for T cells in preventing metastases at distal organs has been demonstrated. Therefore, we examined the impact of C5aR blockade on both of these T cell populations. We found higher numbers of $CD4^+$ and $CD8^+$ T cells in the peripheral blood (Fig. 2A, E) and higher percentages of these cells in the lungs of breast tumor-bearing mice treated with C5aRA compared to control mice (Fig. 2B, F). A similar observation was made in $C5aR^{-/-}$ mice (data not shown). We hypothesize that these cells, which were found to be more frequent in $C5aR^{-/-}$ or C5aRA treated mice, would also be more efficient in the immunosurveillance of the distant organs, eventually contributing to reduction in metastatic burden. This hypothesis is supported by significantly higher percentages of IFN-γ producing $CD4^+$ and $CD8^+$ T cells observed in the lungs of C5aRA treated or $C5aR^{-/-}$ mice when stimulated *ex vivo* with CD3/CD28 antibodies (Fig. 2C, G, D, H). Thus, we propose that the absence of C5aR-signaling encompasses Th1 and Tc1 predominant responses, which are likely to be involved in the clearance of circulating and/or seeding tumor cells in the lungs. This is further supported by significantly higher numbers of perforin-armed $CD8^+$ T cells infiltrating the

lungs of breast tumor-bearing mice that received C5aRA (Fig. 2I, J), supporting contribution of these cells to protection of this organ against metastasizing tumor cells, since acquisition of perforin is a major effector function of $CD8^+$ cytotoxic T cells (CTL) and these cells posses tumoricidal activity (20). The impact of C5aR signaling on T cell accumulation in metastases-targeted organs appears to be indirect, as we did not detect any expression of C5aR on peripheral blood $CD4^+$ and $CD8^+$ T cells (*Supplemental* Fig. S1D). Next, we examined expression of CXCR-3 and LFA-1 on $CD8^+$T cells in peripheral blood of breast tumor-bearing mice treated with C5aRA and PBS, since these receptors are involved in the homing of effector $CD8^+$T cells to the lungs in other models (21-23). However, we found no differences in the expression of these receptors (data not shown). Similar to the lungs, an increased accumulation of CTLs was observed in the livers of $C5aR^{-/-}$ mice compared to Balb/c WT mice (*Supplemental* Fig. S1E, F).

To confirm that reduction in metastatic burden caused by C5aR inhibition was dependent on the protective role of $CD8^+$ T cells, we investigated the impact of C5aR inhibition on lung metastases in mice with depleted $CD8^+$ T cells. C5aR blockade did not reduce lung metastases in these mice (Fig. 2K). On the contrary, in mice with an intact $CD8^+$ T cell population treated with control IgG, we observed a protective effect of C5aRA treatment, with a significant reduction in the lung metastatic burden compared to control mice (Fig. 2K). This observation indicates that C5aR inhibits the protective function of $CD8^+$ T cells in metastasis-targeted organs rendering them unable to control metastasis.

C5a regulates the immunosuppressive environment of metastases-targeted organs

The accumulation of immunosuppressive myeloid cells has been reported to be a contributing factor in the formation of premetastatic sites, thereby facilitating metastasis (5, 6). However, factors regulating the recruitment of these cells to distant sites need to be elucidated. In our previous study in a model of HPV-induced cancer, we demonstrated that C5a acts as a potent chemoattractant of MDSCs to the primary tumors (15). Thus, we hypothesized that C5a/C5aR also activates and recruits MDSCs to premetastatic niches, resulting in immunosuppression in metastases targeted organs prior to tumor cell arrival. In fact, genetic (Fig. 3A) and pharmacological (Fig. 3B, C) ablation of C5aR decreased MDSC infiltration of the lungs of breast tumor-bearing mice (Fig. 3A, B, C). A similar reduction in MDSCs was observed in the livers of $C5aR^{-/-}$ mice (*Supplemental* Fig. S1 G, H). We did not find any differences in the numbers of MDSCs present in peripheral blood (*Supplemental* Fig. S2 A) and bone marrow (*Supplemental* Fig. S2 B) of C5aRA-treated and control mice. In an independent set of experiments, we determined that tumor cells were first observed in the lungs between days 20 to 26 after injection of 4T1 cells (*Supplemental* Fig. S2 C), whereas a significant increase in MDSC infiltration into the lungs could be detected at day 16 (*Supplemental* Fig. S2 D, E). Interestingly, we observed that complement activation, which is associated with C5a generation, occurred in the lungs of breast tumor-bearing mice prior to metastases and significant accumulation of MDSC (Fig. 3D), since complement C3 fragments were deposited in the lungs as early as at day 4 after tumor implantation (Fig. 3D). Therefore, we propose that in premetastatic niches, C5a functions as a chemoattractant for

MDSCs expressing high levels of C5aR (Fig. 3E). This hypothesis is supported by the presence of high amounts of C5a in peripheral blood of breast tumor-bearing mice, which increased at later time points (*Supplemental* Fig. S3A). Although we observed some increases in C5a levels in BAL, these differences did not reach statistical significance (data not shown). Interestingly, we also found increases in total C3 concentration in plasma (*Supplemental* Fig. S3B) and BAL (*Supplemental* Fig. S3C) suggesting enhanced production of complement fragments in tumor-bearing mice. Increased expression of genes encoding C3 and C5 in the liver (*Supplemental* Fig. S3D) indicated that this organ is a primary site of C3 and C5 production in tumor-bearing mice. In contrast, we did not observe increased expression of C3 and C5 in the lungs (data not shown). Importantly, we did not find enhanced deposition of C3 cleavage fragments and increased expression of C3 and C5 genes (data not shown) in the kidneys that are usually spared from metastasis in this tumor model (16). We observed deposition of some C3 cleavage fragments limited to the periphery of kidney glomeruli in tumor-free mice with identical staining pattern as reported previously (24). The presence of primary breast tumors did not increase this deposition (*Supplemental* Fig. S3E), indicating that enhanced complement activation is limited to organs targeted by metastasis.

Since immunosuppressive properties of MDSC in the primary tumor microenvironment are maintained to a large extent by cytokines produced in these cells (25), we investigated whether similar mechanisms operated in premetastatic niches. The impact of C5aR inhibition on the expression of cytokines involved in immunosuppression, such as IL-10, and TGF-β, was evaluated in lung myeloid cells of

tumor-bearing mice. We determined numbers of cells that produced only one of the examined cytokines, as well as cells that co-expressed both cytokines. Total lung cells were isolated from breast tumor-bearing mice treated with C5aRA or PBS and stimulated *ex vivo* with the TLR4 agonist lipopolysaccharide (LPS). We found reduction in the amount of $CD11b^+$ cells producing only TGF-β in mice treated with C5aRA compared to the PBS group (Fig. 3F). Relatively low numbers of cytokine-producing cells were observed in total lung cells. Of note, extremely rare hematopoietic stem cell/progenitors have found to be key contributors to the premetastatic niche (7). Importantly, we found that C5aR inhibition reduced numbers of $CD11b^+$ cells that co-produced TFG-β and IL-10 (Fig. 3G). TGF-β and IL-10, in addition to facilitating metastasis (26, 27), are also reported to promote T_{reg} cell generation (28, 29), thereby suppressing adaptive immunity in the tumor microenvironment (25). Therefore, we next assessed whether decreased production of these cytokines in mice treated with C5aRA correlated with the reduced numbers of T_{reg} cells in the lungs of mice with primary breast tumors. We found that these mice had lower numbers of T_{reg} cells compared to control mice (Fig. 3H). This finding was consistent with a reduction in the numbers of T_{reg} cells in the circulation (Fig. 3I). Thus, we propose that C5aR signaling contributes to immunosuppression in metastases-targeted lungs via recruitment of MDSCs to these sites, regulation of TGF-β and IL-10 expression in these cells and, consequently, generation of T_{reg} cells.

C5aR in MDSCs affects T cell polarization in metastases-targeted organs

We observed that C5aR-deficiency led to Th1 polarization of $CD4^+$ T cells in the lungs of breast tumor-bearing mice (Fig. 4A). To confirm that C5a impacts generation

and polarization of anti-tumor effector T cell responses in metastases-targeted organs by modulating functions of MDSCs, $CD4^+$ T cells isolated from spleens of tumor-free "naïve" mice were differentiated *in vitro* by stimulating with CD3/CD28 antibodies in the presence of lung-derived MDSCs ($CD11b^+Gr\text{-}1^+$) from control or C5aRA-treated breast tumor-bearing mice. Importantly, we observed by FACS analysis that these T cells lacked C5aR expression on their surface, excluding the possibility of a direct action of C5aRA on T cells (*Supplemental* Fig. S1D). We found that $CD4^+$ T cells differentiated in the presence of lung MDSCs from C5aRA-treated mice displayed increased expression of IFN-γ, resulting in a higher Th1/Th2 ratio compared to a similar setting that used lung MDSC from the PBS group (Fig. 4B, C). Based on these data, we propose that C5aR signaling contributes to the polarization of $CD4^+$ T cells to a Th2 type in the lungs of tumor-bearing mice by modulating MDSC functions and that disabling C5aR signaling reverses this effect.

Inflammatory changes in the premetastatic niche resemble interstitial pneumonia-like inflammation

In addition to the decrease in metastatic burden and decreased MDSC infiltration into the lungs and liver, C5aR-deficiecy ($C5aR^{-/-}$) markedly attenuated inflammation in these organs. This was demonstrated by reduced inflammatory infiltrates in intra-alveolar septa in the lungs (Fig. 5A), as well as in periportal areas of the liver (Fig. 5 B). Morphologic heterogeneity in these infiltrates suggests that, apart from MDSCs, other cells contribute to premetastatic niche formation and recruitment of these cells could be C5aR-dependent. A detailed histopathological evaluation revealed progressive inflammatory changes in the intra-alveolar septa of mice bearing tumors. This

inflammation acquired an interstitial ‘pneumonia-like’ pattern in advanced stages (Fig. 5C). The diffuse interstitial infiltrates in the lungs were composed of cells resembling granulocytes, with an admixture of small lymphocytes and histiocytes. Occasionally, immature myeloid cells were noted (Fig. 5D).

In the next set of experiments, we verified that inflammatory alterations of the lungs, observed prior to metastasis in the breast tumor-bearing mice, facilitated seeding of these organs by circulating tumor cells. In these experiments, mice were injected with regular 4T1 cells into the mammary fat pad to create premetastatic niche in the lungs, then these mice and tumor-free control mice were injected i.v. with 4T1-GFP$^+$ (GFP-expressing) cells. This experimental approach was used to investigate whether lung inflammation associated with, and induced by, the primary breast tumor could facilitate lung seeding by circulating GFP$^+$ 4T1 cells (injected i.v.). Colonization of lungs by circulating tumor cells is reported to depend upon existence of a premetastatic niche. We observed that lung inflammation in tumor-bearing mice increased seeding of 4T1-GFP$^+$ cells in this organ, evident from higher numbers and increased sizes of GFP$^+$ metastases in the lungs of mice previously injected with regular 4T1 into the mammary fat pad (Fig. 5E, F, G, H). Nevertheless, GFP$^-$ (non-fluorescent) metastases were also present in these mice (Fig. 5E) but, by using animal imaging combined with fluorescent microscopy, we were able to distinguish GFP$^+$ from GFP$^-$ metastases. When these experiments were repeated with 10-fold lower numbers of 4T1-GFP$^+$ cells injected i.v., only mice bearing breast tumors developed GFP$^+$ metastases in their lungs (Fig. 5I), indicating that circulating tumor cells required prior inflammatory changes in the premetastatic niche before effective lung seeding.

Complement deposition associated with MDSC recruitment may contribute to premetastatic niche formation in breast cancer patients

To determine the clinical significance of our findings, sections of TDLNs from breast cancer patients with invasive, not-otherwise specified (NOS), ductal carcinoma were examined for infiltration by MDSCs and for complement activation (Fig. 6A, B). In these experiments, MDSCs were identified by co-expression of $CD11b^+$ and $CD33^+$ and complement deposition was analyzed as C3 cleavage product deposition (Fig. 6A, B). We found accumulation of MDSCs in the TDLNs with breast tumor metastases, as well as in those that were free of metastases, suggesting a correlation with and possible involvement of MDSCs in formation of premetastatic niches in humans. We observed C5aR-expression in those areas occupied by MDSCs (*Supplemental* Fig. S3F). Moreover, complement activation in the TDLNs was observed as extracellular deposition of C3 cleavage fragments in the vasculature and sinuses of these lymph nodes (Fig. 6B). In addition, we observed production of C3 in the macrophages located in sinuses, as demonstrated by intracellular staining (Fig. 6B). Intriguingly, both complement deposition and local production of C3 appeared to be higher in the TDLNs where metastases were present (Fig. 6B, right panels vs. left panels).

Discussion

The role of complement in cancer remains uncertain with only a few studies to date reporting on tumor-promoting or tumor-inhibiting properties of complement proteins (30). Recent studies have provided some, albeit limited, mechanistic insights into the roles of certain complement proteins in cancer progression. For example, C5a

overexpression in tumor cells has been linked to tumor regression in a mouse model of breast cancer (31). Conversely, C5a has also been shown to promote progression of cancer in a model of cervical cancer through the recruitment of MDSCs to tumors (15). The activation of MDSC in the tumor microenvironment by C5aR leads to production of reactive oxygen and nitrate species that inhibit anti-tumor T cell responses (12, 15, 32). These findings placed C5a among inflammatory mediators implicated in the progression of cancer (33). In addition, recent work in a transgenic model of ovarian cancer has shown the contribution of complement to angiogenesis in ovarian tumors. In the absence of complement factor C3 or C5aR, the transgenic mice either did not develop ovarian tumors or the growth of tumors was significantly limited (34).

Our present study reveals a new role for C5a and C5aR in tumor metastasis. We propose that C5a/C5aR signaling contributes to an inflammatory condition that creates a premetastatic niche environment by recruiting and facilitating generation of immunosuppressive cells in the lungs and livers of mice with breast malignancy. Recent studies have identified some key components of premetastatic niches and potential mechanisms that are involved in tumor cell recruitment to distal sites targeted by metastases (5, 7, 8, 10). However, considering that several other factors may be involved in this process, regulation of premetastatic niche environment and its role in metastases requires further elucidation. It is for example not known why different types of tumor cells home to different organs (35). Although accumulation of immunosuppressive MDSCs cells in a premetastatic niche was previously demonstrated, the precise mechanism governing this recruitment and the role of immunosuppression in facilitating metastases remain unclear (13). The present study

addresses this gap in knowledge of the properties of premetastatic niches. Furthermore, the roles of effector T cells in preventing metastasis at distant sites remain unknown. To our knowledge, this is the first report demonstrating that blockade of C5aR signaling enables $CD8^+$ T cells to control lung metastases. In addition, our study suggests a protective nature for Th1/Tc1 polarized $CD4^+$/$CD8^+$ T cells in the context of lung metastasis. These findings have important therapeutic implications, as they provide proof of concept that boosting type 1 $CD4^+$ T cell and CTL responses, with simultaneous targeting of the mechanisms of immunosuppression, can prevent metastases even at an advanced stage of cancer.

In addition, given the abundance of complement fragments in plasma and interstitial fluid and their function in maintaining immune homeostasis (36), the contributions of complement C5a/C5aR signaling to premetastatic inflammation described herein points to a previously unknown mechanism for metastasis, which can operate at various locations. This is further supported by ubiquitous production of complement fragments by virtually all cells in the body participating in the innate immune responses, thus accessibility of complement proteins in most of the tissues is very high (36). Complement activation can also occur *in vitro*, for instance, complement components were secreted when $CD4^+$ T cells were co-cultured with dendritic cells (37, 38), indicating that formation of immunological synapses between proximal immune cells is sufficient enough to produce and activate complement fragments. Our data has shown that activation of complement in lungs of mice occurred as early as day 4 after injection of tumor cells and was associated with high concentrations of C5a in plasma. We observed an increase in C3 concentrations in plasma and BAL indicating increased

production of C3. In addition, we found a significant increase in C3 and C5 mRNA levels in the liver after 4T1 tumor inoculation. Therefore, we conclude that an increased concentration of complement fragments in the circulation of tumor-bearing mice is a consequence of increased production in the liver. This rapid onset of activation of the complement cascade is an upstream regulator of the premetastatic niche. C5a generated in this cascade leads to recruitment of MDSCs to the lungs prior to metastases. This function of C5a is similar to its role in recruiting leukocytes to sites of inflammation (14). Given ubiquitous expression of C5aR on cells of myeloid-origin, other myeloid cells in addition to MSDCs are also likely to be recruited to the premetastatic lungs. Interestingly, the morphological pattern of lung infiltration resembled that of interstitial pneumonia with most of the infiltrating cells present in the intra-alveolar septa. This type of pneumonitis in humans is difficult to diagnose based on physical examination, however, chest x-ray showing diffuse alveolar opacities or computerized tomography may provide diagnostic clues to premetastatic inflammation.

In addition to recruiting MDSCs, C5a/C5aR signaling stimulated TGF-β and IL-10 production in these cells. Since co-expression of TGF-β and IL-10 contributes to T_{reg} cell generation upon antigenic stimulation (29), we speculate that C5aR signaling in recruited MDSCs regulates this process in premetastatic sites. Our data contrast with recent studies demonstrating inhibitory functions of C5aR in T_{reg} cell generation (38, 39). This “discordance” is consistent with immunomodulatory functions of C5aR being highly context dependent. In contrast to our study, the previous work was conducted in non-tumor models (38-40). In addition, some studies focused on thymus-derived (natural) T_{reg} cells (39) that are generated through different pathways compared to

inducible T_{reg} cells (41, 42). It appears that primary tumors alter the immune microenvironment, including the cytokine milieu, to such an extent that C5aR signaling in tumor-bearing mice has opposing roles to those in non-tumor models. Our previous work in a model of HPV-induced cancer has shown that C5aR inhibits antitumor T cell responses, although this study has examined roles of C5aR only in primary tumors and not at sites distal to the tumors (15).

Inhibitory roles of complement in T_{reg} cell generation have also been suggested in a transgenic model of ovarian cancer (34). Although MDSCs have been shown to increase T_{reg} cell generation (43) and T_{reg} cells and MDSCs are known for their immunosuppressive properties in the primary tumors (44), roles of these cells at the sites targeted by metastases have not been demonstrated. We propose that MDSCs and T_{reg} cells have similar functions in metastases-targeted organs and work together to shield metastasizing tumor cells from immune attack. Indeed, reduction in MDSCs and T_{reg} cells in the lungs of mice with breast tumors treated with C5aRA was associated with $CD4^+$ and $CD8^+$ T cell responses that resulted in reduced metastasis to the lungs. The lack of impact of C5aR inhibition on metastases in mice that were devoid of $CD8^+$ T cells demonstrated that C5aR signaling facilitates metastasis by suppressing $CD8^+$ T cell responses. Moreover, considering that type 1 $CD4^+$ T cell responses are helpful in generating anti-tumor $CD8^+$ T cell responses in the primary tumor microenvironment, we analyzed $CD4^+$ T cell function in the lungs of breast tumor-bearing mice. We observed that disabling C5aR signaling augments IFN-γ and lowers IL-4 expression in $CD4^+$ T cells in the lungs of mice compared to the control group. Further, to prove that the difference in T cell polarization was attributed to recruitment of MDSC, experiments

were conducted to differentiate “naïve” $CD4^+$ T cells into effectors in the presence of lung MDSC isolated from C5aRA treated and control mice. These studies suggested that C5aR blockade in MDSCs increased numbers of IFN-γ-expressing $CD4^+$ T cells and reduced numbers of IL-4 producing $CD4^+$ T cells. Thus, by using *in vitro* co-culture experiments, we demonstrated that C5a/C5aR affects $CD4^+$ T cell polarization through the modulation of MDSC functions. Nonetheless, besides improving the functional quality of T cells, C5aR blockade also resulted in increased recruitment of these cells to the lungs.

The expression of C5aR on T cells remains controversial, with conflicting reports on C5aR expression in T cells (45). We did not detect C5aR expression on $CD4^+$ and $CD8^+$ T cells. Therefore, we propose an indirect regulation of T cell responses in the lungs through C5aR. C5aR inhibition did not affect expression of CXCR-3 and LFA-1 on circulating T cells, suggesting that increased T cell homing to the lungs is less likely to be responsible for increased numbers of T cells in the lungs of mice lacking C5aR or treated with C5aRA. A more plausible explanation is that reduction in MDSCs, caused by the lack C5aR signaling, decreases apoptosis and increases survival of T cells, as recent studies have shown that MDSCs promote T cells apoptosis (46). Importantly, effects of C5aR inhibition on metastasis and anti-tumor immunity appear to be independent from mechanisms operating in primary tumors, as this inhibition did not significantly affect growth of tumors in this breast tumor model. This finding, which contrasts with our previous report (15), can be attributed to the higher rate of tumor growth in a breast cancer model compared to the model used previously or simply to the difference in tumor type. The 4T1 tumors were on average three times larger

between day 25 and 27 (time of sacrifice in the current study) after injection of tumor cells, in comparison to TC-1 tumors in the previous study. We assumed that in a case of 4T1 breast tumors, therapy introduced just two weeks before mice were sacrificed was unable to reduce growth of these aggressive tumors.

In conclusion, this study provides evidence for the role of C5a/C5aR signaling in promoting metastasis via immunosuppression in premetastatic sites. Importantly, pharmacological blockade of this receptor efficiently activated adaptive immune responses and reduced lung metastatic burden. Given that the C5aR antagonist used in this study has already progressed to phase 2 clinical trials for inflammatory diseases (17, 47), this report builds an early foundation for introducing C5aR antagonism as a possible means of reducing risk of cancer metastasis in future clinical studies.

Authors' contributions

S.V., N.K.C., and S.K.S. performed all experiments, contributed to the study design, analyzed data and contributed to writing the manuscript. P.S., C.C., and L.R. contributed to *in vivo* studies. S.M. contributed to qPCR studies and data analysis. D.P.F. provided C5aR antagonist, analyzed and interpreted data and revised the manuscript. W.G. interpreted histology of premetastatic organs, analyzed data and revised the manuscript. O.A. provided sections of lymph nodes from breast cancer patients, interpreted histology and immunohistochemistry data and revised the manuscript. M.K. contributed to the study design, analyzed and interpreted data and

revised the manuscript. M.M.M. designed and supervised the study, analyzed and interpreted data and contributed to writing the manuscript.

Grant Support

This research was supported by the Australian NHMRC (456060, 1028423), ARC (DP130100629, CE140100011) and NHMRC SPR Fellowship 1027369 to D.P.F., Cancer Prevention and Research Institute of Texas RP 120168 to M.K., and the Department of Defense Breast Cancer Research Program BC 111038 to M.M.M. Views and opinions of, and endorsements by the author(s) do not reflect those of the US Army or the Department of Defense.

References

1. Weigelt B, Peterse JL, van 't Veer LJ. Breast cancer metastasis: markers and models. Nat Rev Cancer. 2005;5:591-602.
2. Gupta GP, Massague J. Cancer metastasis: building a framework. Cell. 2006;127:679-95.
3. Fidler IJ. The pathogenesis of cancer metastasis: the 'seed and soil' hypothesis revisited. Nat Rev Cancer. 2003;3:453-8.
4. Kaplan RN, Rafii S, Lyden D. Preparing the "soil": the premetastatic niche. Cancer Res. 2006;66:11089-93.
5. Yan HH, Pickup M, Pang Y, Gorska AE, Li Z, Chytil A, et al. Gr-1+CD11b+ myeloid cells tip the balance of immune protection to tumor promotion in the premetastatic lung. Cancer Res. 2010;70:6139-49.
6. Gao D, Joshi N, Choi H, Ryu S, Hahn M, Catena R, et al. Myeloid progenitor cells in the premetastatic lung promote metastases by inducing mesenchymal to epithelial transition. Cancer Res. 2012;72:1384-94.
7. Kaplan RN, Riba RD, Zacharoulis S, Bramley AH, Vincent L, Costa C, et al. VEGFR1-positive haematopoietic bone marrow progenitors initiate the pre-metastatic niche. Nature. 2005;438:820-7.
8. Hiratsuka S, Nakamura K, Iwai S, Murakami M, Itoh T, Kijima H, et al. MMP9 induction by vascular endothelial growth factor receptor-1 is involved in lung-specific metastasis. Cancer Cell. 2002;2:289-300.
9. Sceneay J, Chow MT, Chen A, Halse HM, Wong CS, Andrews DM, et al. Primary Tumor Hypoxia Recruits CD11b+/Ly6Cmed/Ly6G+ Immune Suppressor Cells and

Compromises NK Cell Cytotoxicity in the Premetastatic Niche. Cancer Res. 2012;72:3906-11.

10. Hiratsuka S, Watanabe A, Sakurai Y, Akashi-Takamura S, Ishibashi S, Miyake K, et al. The S100A8-serum amyloid A3-TLR4 paracrine cascade establishes a pre-metastatic phase. Nat Cell Biol. 2008;10:1349-55.
11. Deng J, Liu Y, Lee H, Herrmann A, Zhang W, Zhang C, et al. S1PR1-STAT3 signaling is crucial for myeloid cell colonization at future metastatic sites. Cancer Cell. 2012;21:642-54.
12. Gabrilovich DI, Nagaraj S. Myeloid-derived suppressor cells as regulators of the immune system. Nat Rev Immunol. 2009;9:162-74.
13. Sceneay J, Smyth MJ, Moller A. The pre-metastatic niche: finding common ground. Cancer and Metastasis Reviews. 2013.
14. Markiewski MM, Lambris JD. The role of complement in inflammatory diseases from behind the scenes into the spotlight. Am J Pathol. 2007;171:715-27.
15. Markiewski MM, DeAngelis RA, Benencia F, Ricklin-Lichtsteiner SK, Koutoulaki A, Gerard C, et al. Modulation of the antitumor immune response by complement. Nat Immunol. 2008;9:1225-35.
16. Pulaski BA, Ostrand-Rosenberg S. Mouse 4T1 breast tumor model. Curr Protoc Immunol. 2001;Chapter 20:Unit 20 2.
17. Monk PN, Scola AM, Madala P, Fairlie DP. Function, structure and therapeutic potential of complement C5a receptors. Br J Pharmacol. 2007;152:429-48.

18. Lim J, Iyer A, Suen JY, Seow V, Reid RC, Brown L, et al. C5aR and C3aR antagonists each inhibit diet-induced obesity, metabolic dysfunction, and adipocyte and macrophage signaling. FASEB J. 2013;27:822-31.
19. Reid RC, Abbenante G, Taylor SM, Fairlie DP. A convergent solution-phase synthesis of the macrocycle Ac-Phe-[Orn-Pro-D-Cha-Trp-Arg], a potent new antiinflammatory drug. J Org Chem. 2003;68:4464-71.
20. Kagi D, Vignaux F, Ledermann B, Burki K, Depraetere V, Nagata S, et al. Fas and perforin pathways as major mechanisms of T cell-mediated cytotoxicity. Science. 1994;265:528-30.
21. Seung E, Cho JL, Sparwasser T, Medoff BD, Luster AD. Inhibiting CXCR3-dependent CD8+ T cell trafficking enhances tolerance induction in a mouse model of lung rejection. J Immunol. 2011;186:6830-8.
22. Holt PG, Strickland DH, Wikstrom ME, Jahnsen FL. Regulation of immunological homeostasis in the respiratory tract. Nat Rev Immunol. 2008;8:142-52.
23. Thatte J, Dabak V, Williams MB, Braciale TJ, Ley K. LFA-1 is required for retention of effector CD8 T cells in mouse lungs. Blood. 2003;101:4916-22.
24. Paixao-Cavalcante D, Hanson S, Botto M, Cook HT, Pickering MC. Factor H facilitates the clearance of GBM bound iC3b by controlling C3 activation in fluid phase. Mol Immunol. 2009;46:1942-50.
25. Ostrand-Rosenberg S, Sinha P, Beury DW, Clements VK. Cross-talk between myeloid-derived suppressor cells (MDSC), macrophages, and dendritic cells enhances tumor-induced immune suppression. Seminars in Cancer Biology. 2012;22:275-81.

26. Massague J. TGFbeta signalling in context. Nat Rev Mol Cell Biol. 2012;13:616-30.
27. Padua D, Massague J. Roles of TGFbeta in metastasis. Cell Research. 2009;19:89-102.
28. Shevach EM. Mechanisms of foxp3+ T regulatory cell-mediated suppression. Immunity. 2009;30:636-45.
29. Chen W, Jin W, Hardegen N, Lei KJ, Li L, Marinos N, et al. Conversion of peripheral CD4+CD25- naive T cells to CD4+CD25+ regulatory T cells by TGF-beta induction of transcription factor Foxp3. J Exp Med. 2003;198:1875-86.
30. Markiewski MM, Lambris JD. Is complement good or bad for cancer patients? A new perspective on an old dilemma. Trends Immunol. 2009;30:286-92.
31. Kim DY, Martin CB, Lee SN, Martin BK. Expression of complement protein C5a in a murine mammary cancer model: tumor regression by interference with the cell cycle. Cancer Immunol Immunother. 2005;54:1026-37.
32. Ostrand-Rosenberg S. Cancer and complement. Nat Biotechnol. 2008;26:1348-9.
33. Balkwill FR, Mantovani A. Cancer-related inflammation: Common themes and therapeutic opportunities. Seminars in Cancer Biology. 2012;22:33-40.
34. Nunez-Cruz S, Gimotty PA, Guerra MW, Connolly DC, Wu YQ, DeAngelis RA, et al. Genetic and pharmacologic inhibition of complement impairs endothelial cell function and ablates ovarian cancer neovascularization. Neoplasia. 2012;14:994-1004.
35. Joyce JA, Pollard JW. Microenvironmental regulation of metastasis. Nat Rev Cancer. 2009;9:239-52.
36. Ricklin D, Hajishengallis G, Yang K, Lambris JD. Complement: a key system for immune surveillance and homeostasis. Nat Immunol. 2010;11:785-97.

37. Strainic MG, Liu J, Huang D, An F, Lalli PN, Muqim N, et al. Locally produced complement fragments C5a and C3a provide both costimulatory and survival signals to naive CD4+ T cells. Immunity. 2008;28:425-35.
38. Strainic MG, Shevach EM, An F, Lin F, Medof ME. Absence of signaling into CD4(+) cells via C3aR and C5aR enables autoinductive TGF-beta1 signaling and induction of Foxp3(+) regulatory T cells. Nat Immunol. 2013;14:162-71.
39. Kwan WH, van der Touw W, Paz-Artal E, Li MO, Heeger PS. Signaling through C5a receptor and C3a receptor diminishes function of murine natural regulatory T cells. J Exp Med. 2013;210:257-68.
40. Weaver DJ, Jr., Reis ES, Pandey MK, Kohl G, Harris N, Gerard C, et al. C5a receptor-deficient dendritic cells promote induction of Treg and Th17 cells. Eur J Immunol. 2010;40:710-21.
41. Wing K, Sakaguchi S. Regulatory T cells exert checks and balances on self tolerance and autoimmunity. Nat Immunol. 2010;11:7-13.
42. Banerjee A, Vasanthakumar A, Grigoriadis G. Modulating T regulatory cells in cancer: how close are we? Immunol Cell Biol. 2013;91:340-9.
43. Huang B, Pan PY, Li Q, Sato AI, Levy DE, Bromberg J, et al. Gr-1+CD115+ immature myeloid suppressor cells mediate the development of tumor-induced T regulatory cells and T-cell anergy in tumor-bearing host. Cancer Research. 2006;66:1123-31.
44. Marigo I, Dolcetti L, Serafini P, Zanovello P, Bronte V. Tumor-induced tolerance and immune suppression by myeloid derived suppressor cells. Immunological Reviews. 2008;222:162-79.

45. Dunkelberger J, Zhou L, Miwa T, Song WC. C5aR expression in a novel GFP reporter gene knockin mouse: implications for the mechanism of action of C5aR signaling in T cell immunity. J Immunol. 2012;188:4032-42.
46. Yu J, Du W, Yan F, Wang Y, Li H, Cao S, et al. Myeloid-derived suppressor cells suppress antitumor immune responses through IDO expression and correlate with lymph node metastasis in patients with breast cancer. J Immunol. 2013;190:3783-97.
47. Kohl J. Drug evaluation: the C5a receptor antagonist PMX-53. Curr Opin Mol Ther. 2006;8:529-38.

Figure legends

Figure 1. C5aR signaling promotes metastasis to the lungs of breast tumor-bearing mice. Scans of hematoxylin and eosin (H&E) stained sections of the lungs of wild-type (WT) and C5aR-deficient ($C5aR^{-/-}$) mice with breast tumors (upper panels) and their corresponding digital mark-up images (lower panel), metastases-purple, tissue with severe inflammatory changes-red, and remaining tissue-yellow and pink colorations (**A**). Quantification of lung metastases from A, **P*=0.0421 (t-test) (**B**). Breast tumor volumes of WT and $C5aR^{-/-}$ mice at various time points after tumor cell injection (**C**). GFP^{+} metastases in the lungs of tumor-bearing mice treated with PBS or C5aR antagonist (C5aRA), arrow points to small metastatic tumor (**D**). Number of lung metastases, **P*=0.0225 (Mann Whitney test) (**E**), and area covered by these metastases **P*=0.0141 (Mann Whitney test) (**F**), in PBS and C5aRA-treated tumor-bearing mice. Breast tumor

volumes of WT Balb/c mice treated with C5aRA or PBS at various time points after injection of tumor cells (**G**). Horizontal lines represent mean in scatter plots (**C, E-G**). Bars represent mean + s.e.m. Data are representative of two independent experiments with n_1=19, n_2=10 (**A-C**), or two independent experiments with $n_1 \geq 8$, n_2=10 (**D-G**).

Figure 2. C5a receptor blockade enhances $CD4^+$ and $CD8^+$ T cell responses. $CD4^+$ T cells from peripheral blood, **P*=0.0358 (t-test) (**A**), and lungs, **P*=0.2452, with 95% confidence interval (CI) -0.08 to 0.30 (t-test) (**B**), of breast tumor-bearing mice iγnjected with PBS or C5aR antagonist (C5aRA). IFN-γ expressing $CD4^+$ T-cells from lungs of breast tumor-bearing mice injected with PBS or C5aRA, **P*=0.0368 (t-test) (**C**), and WT and $C5aR^{-/-}$ mice, **P*=0.0004 (t-test) (**D**). $CD8^+$ T cells from peripheral blood, **P*=0.0267 (t-test) (**E**), and lungs of breast tumor-bearing mice injected with PBS or C5aRA, **P*=0.0471(t-test) (**F**). IFN-γ expressing $CD8^+$ T cells from lungs of breast tumor-bearing mice injected with PBS and C5aRA, **P*=0.1438, 95% CI -0.01 to 0.002 (t-test) (**G**), and WT and $C5aR^{-/-}$ mice **P*=0.0364 (Mann Whitney test) (**H**). Perforin-expressing (red fluorescence) $CD8^+$ (green fluorescence) T cells in lungs of breast tumor-bearing mice injected with PBS (left) or C5aRA (two right panels) (**I**), with quantification **P*=0.0008 (t-test) (**J**). Lung metastatic burden in Balb/c WT mice treated with C5aRA or PBS and injected with CD8-neutralizing antibody or isotype IgG, **P*=0.0005 (Mann Whitney test), not significant (n.s) (**K**). $CD8^+$ T cells in peripheral blood of Balb/c WT mice treated with PBS or C5aRA and injected with CD8-neutralizing antibody (α-CD8) or isotype IgG (Isotype), **P*=0.0057 (Mann Whitney test), ***P*=0.0040 (t-test with Welch's correction) (**L**). Scale bar 20 μm. Bars represent mean + s.e.m. Data are representative of two

independent experiments, n_1=9 and n_2=10 (**A, B, C, F, G**) or three independent experiments n_1=8, n_2=9 and n_3=10 (**E**), or one experiment with at least *n*=8 (**D-H**, **I-L**).

Figure 3. C5aR-mediated immunosuppression in the lungs of breast tumor-bearing mice. CD11b and Gr-1 expression, green and red fluorescence, respectively, in lung MDSCs of tumor-bearing wild-type (WT) and $C5aR^{-/-}$ mice (**A**), and tumor-bearing WT mice injected with PBS or C5aR antagonist (C5aRA) (**B**). MDSCs quantification, **P*=0.0017 (t-test) from B (**C**). C3 cleavage products in the lungs of tumor-free and tumor-bearing mice (**D**). C5aR expression in $CD11b^+$ blood cells in tumor-bearing mice (**E**). Percentages of $CD11b^+$ cells expressing TGF-β after *ex vivo* LPS stimulation, **P*=0.0085 (t-test with Welch's correction) (**F**), and co-expressing TGF-β and IL-10, **P*=0.0412 (t-test with Welch's correction) (**G**) in the lungs of tumor-bearing mice injected with PBS or C5aRA. Percentages of T_{reg} cells in the lungs, **P*=0.2679, 95% CI -0.001 to 0.005 (t-test) (**H**), and absolute counts of T_{reg} cells in the peripheral blood, **P*=0.05 (t-test) (**I**) of tumor-bearing mice injected with PBS or C5aRA. Blue fluorescence-DAPI (**A, B, D**). Bars represent mean + s.e.m. Data are representative of one experiment with *n*=8 (**A**); or two independent experiments, n_1≥8 and n_2=10 (**B, C, E**); or two independent experiments, n_1=3 and n_2=8 (**D**); or one experiment, *n*=9 (**F, G**); or one experiment, *n*≥5 (**H**, **I**). Scale bar-100μm for A**,** B**,** 200μm for D, and 50μm for D.

Figure 4. C5aR impacts T cell polarization by regulating lung MDSCs. Th1/Th2 ratio calculated from IFN-γ (Th1)- and IL-4 (Th2)-expressing $CD4^+$ T cells obtained from the lungs of breast tumor-bearing wild-type (WT) and $C5aR^{-/-}$ mice, **P*=0.0245 (t-test with Welch's correction) (**A**). Percentages of IFN-γ, **P*=0.2712, 95% CI -0.02 to 0.06 (t-

test) (**B**), and IL-4 expressing, *P=0.1332, 95% CI -60.23 to 10.18 (t-test with Welch's correction) (**C**) $CD4^+$ T cells differentiated *in vitro* by anti-CD3/CD28 stimulations in the presence of lung MDSCs from breast tumor-bearing mice treated with C5aRA or PBS. Horizontal lines represent mean + s.e.m. Data are representative of one independent experiment with n≥9 (**A**) and n≥5 (**B, C**).

Figure 5. C5aR mediated inflammation facilitates metastases. Hematoxylin and eosin (H&E) stained sections of the lungs of wild-type (WT) and $C5aR^{-/-}$ tumor-bearing mice. Double-headed yellow arrows point to 54.92 µm in WT and 37.61 µm in $C5aR^{-/-}$ mice showing thickness of alveolar septa (**A**). H&E stained sections of the livers of WT and $C5aR^{-/-}$ tumor-bearing mice. Arrows point inflammatory cells (**B**). H&E stained sections of the lungs of tumor-free mice (left panel) and tumor-bearing mice (right panel) (**C**). Immature myeloid cells in H&E stained lung sections of tumor-bearing mice-arrows (**D**). The lungs from tumor-free (left panel) and tumor-bearing mice (right panel) injected i.v. with GFP^+ tumor cells. Upper panel - white light images, note multiple gross metastases in breast tumor-bearing mice, lower panel - fluorescence images, arrows point to few GFP^+ metastases in tumor-free mice, note numerous GFP^+ metastases in breast tumor-bearing mice (**E**). GFP^+ tumor cells (green fluorescence) in sections of the lungs of tumor-free (upper panel) and tumor-bearing mice (lower panel) injected i.v. with GFP^+ tumor cells (**F**). Numbers of GFP^+ metastases in the lungs of tumor-free (TF) and tumor-bearing mice (TB) injected i.v. with GFP^+ tumor cells, *P=0.0604, 95% CI -18.1 to 0.5 (t-test) (**G**). Size (area) of GFP^+ metastases in the lungs of TF & TB mice injected i.v. with GFP^+ tumor cells, *P=0.0159 (Mann Whitney test) (**H**). Bars represent mean + s.e.m. Scans of the end-point H&E stained lung sections from TF (left image) and TB

mice (middle image) injected i.v. with GFP^+ tumor cells. Arrows point to metastases. Inset depicts the enlarged lung area with metastases. Right image-immunohistochemistry detection of GFP in lung metastases (**I**). Data are representative of two independent experiments with n_1=5 and n_2=6 (**A, B,** and **E-I**), or two independent experiments with n_1=3 and n_2=8 (**C, D**). Scale bars-100μm except 50 μm for D.

Figure 6. MDSC infiltration and C3 deposition and expression in lymph nodes (LN) of breast cancer patients. Immunohistochemistry detection of human MDSC markers CD11b (brown) and CD33 (fast red) in axillary lymph nodes with (LN+) or without (LN-) breast cancer metastases. Yellow in digital mark-up images indicates cells that coexpress both CD11b and CD33 (**A**). Immunohistochemistry detection of C3/C3c in LN+ and LN-. Frames outline areas, which are shown in higher magnification in panels below. Arrowheads point to vessels with C3 cleavage product deposition, Arrows point to macrophages producing C3 (**B**). Scale bars-200μm for (**A**); 400μm, 200μm, and 50μm for B upper, middle, and lower panel respectively. Data are representative of 12 patients diagnosed with breast non-otherwise specified (NOS) ductal carcinoma with axillary lymph node metastases (six patients) and without axillary lymph node involvement (six patients) (**A, B**).

Figure 1

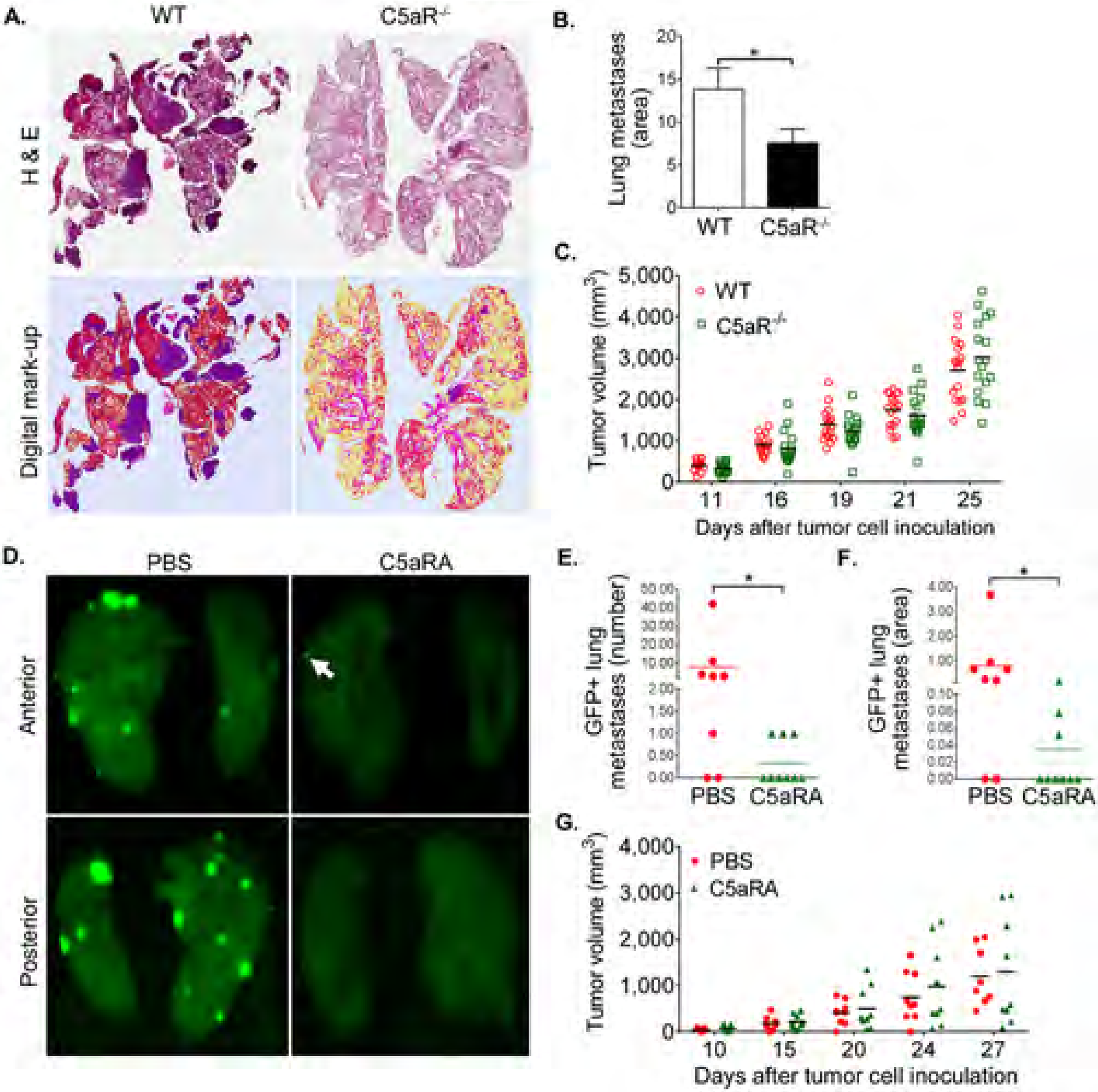
A.
WT
C5aR-/-
H & E
Digital mark-up
B.
Lung metastases (area)
20
15
10
5
0
*
WT
C5aR-/-
C.
Tumor volume (mm3)
5,000
4,000
3,000
2,000
1,000
0
WT
C5aR-/-
11
16
19
21
25
Days after tumor cell inoculation
D.
PBS
C5aRA
Anterior
Posterior
E.
GFP+ lung metastases (number)
50.00
40.00
30.00
20.00
10.00
2.00
1.50
1.00
0.50
0.00
*
PBS
C5aRA
F.
GFP+ lung metastases (area)
4.00
3.00
2.00
1.00
0.10
0.08
0.06
0.04
0.02
0.00
*
PBS
C5aRA
G.
Tumor volume (mm3)
4,000
3,000
2,000
1,000
0
PBS
C5aRA
10
15
20
24
27
Days after tumor cell inoculation

Figure 2

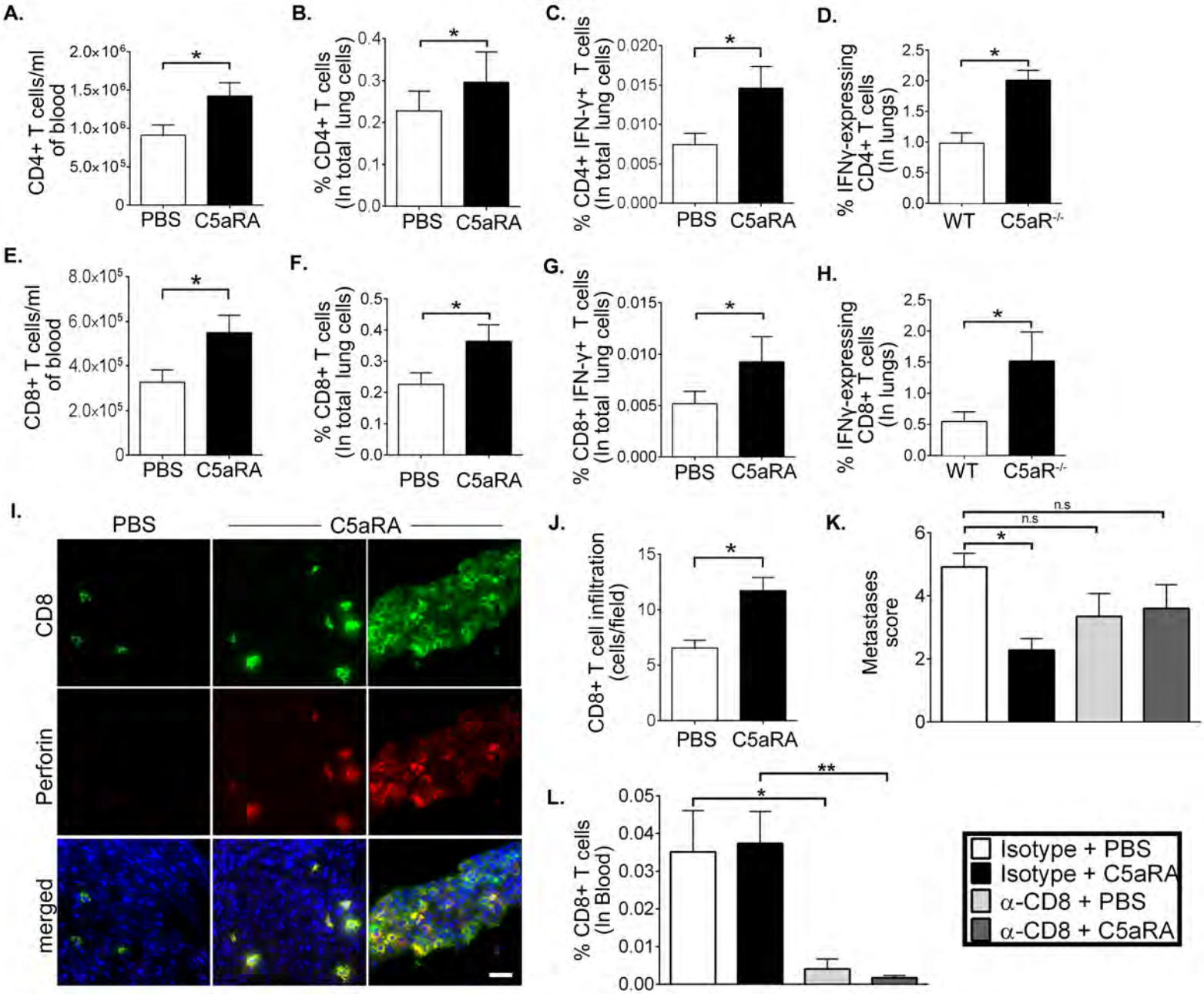
A.
CD4+ T cells/ml of blood
2.0×10^6
1.5×10^6
1.0×10^6
5.0×10^5
0
PBS
C5aRA
B.
% CD4+ T cells (In total lung cells)
0.4
0.3
0.2
0.1
0.0
PBS
C5aRA
C.
% CD4+ IFN-γ+ T cells (In total lung cells)
0.020
0.015
0.010
0.005
0.000
PBS
C5aRA
D.
% IFNγ-expressing CD4+ T cells (In lungs)
2.5
2.0
1.5
1.0
0.5
0.0
WT
C5aR-/-
E.
CD8+ T cells/ml of blood
8.0×10^5
6.0×10^5
4.0×10^5
2.0×10^5
0
PBS
C5aRA
F.
% CD8+ T cells (In total lung cells)
0.5
0.4
0.3
0.2
0.1
0.0
PBS
C5aRA
G.
% CD8+ IFN-γ+ T cells (In total lung cells)
0.015
0.010
0.005
0.000
PBS
C5aRA
H.
% IFNγ-expressing CD8+ T cells (In lungs)
2.5
2.0
1.5
1.0
0.5
0.0
WT
C5aR-/-
I.
PBS
C5aRA
CD8
Perforin
merged
J.
CD8+ T cell infiltration (cells/field)
15
10
5
0
PBS
C5aRA
K.
n.s
n.s
Metastases score
6
4
2
0
L.
% CD8+ T cells (In Blood)
0.05
0.04
0.03
0.02
0.01
0.00
Isotype + PBS
Isotype + C5aRA
α-CD8 + PBS
α-CD8 + C5aRA

Figure 3

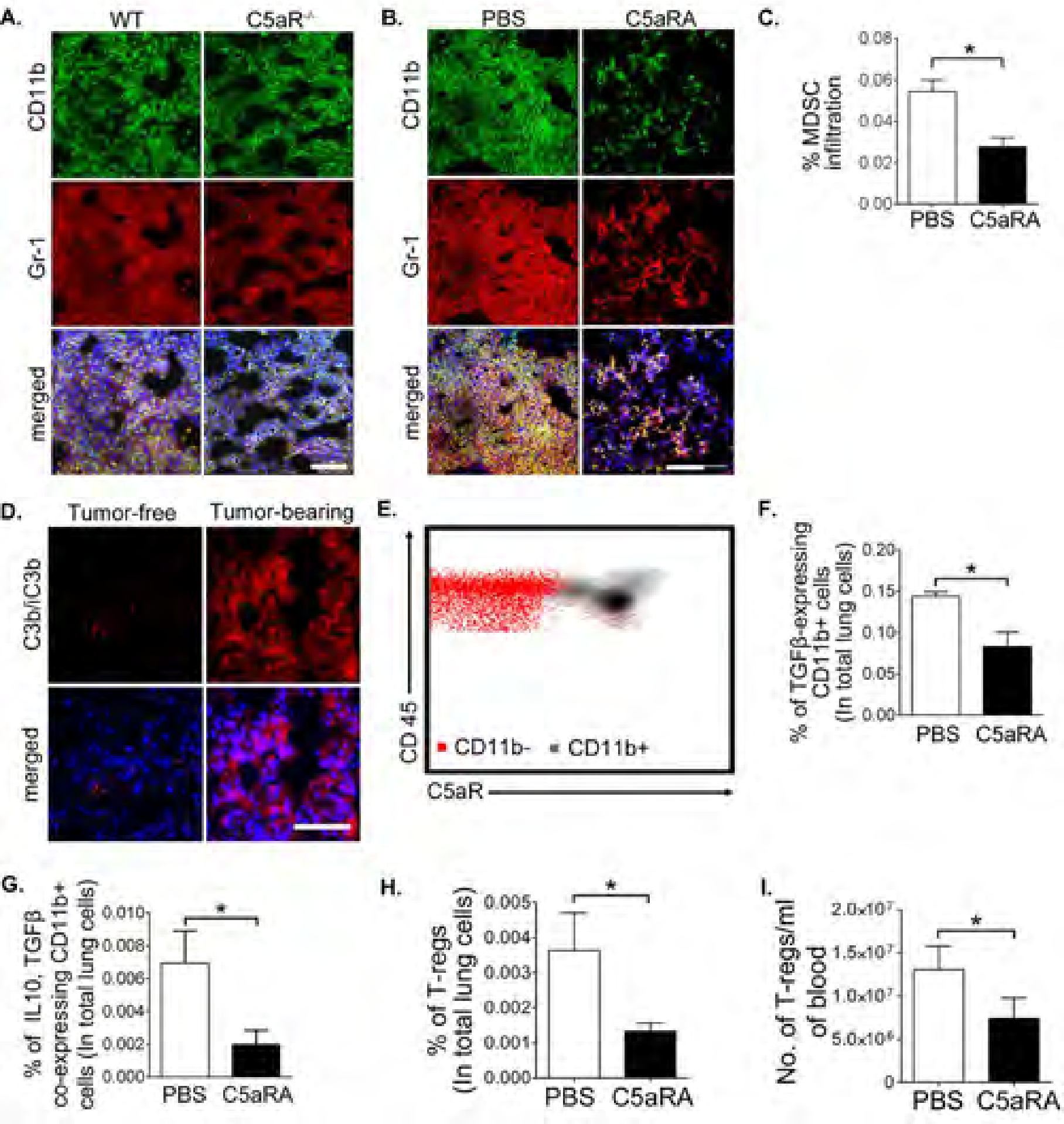
A.
WT
C5aR-/-
CD11b
Gr-1
merged
B.
PBS
C5aRA
CD11b
Gr-1
merged
C.
% MDSC infiltration
0.08
0.06
0.04
0.02
0.00
*
PBS
C5aRA
D.
Tumor-free
Tumor-bearing
C3b/iC3b
merged
E.
CD 45
CD11b-
CD11b+
C5aR
F.
% of TGFβ-expressing CD11b+ cells (In total lung cells)
0.20
0.15
0.10
0.05
0.00
*
PBS
C5aRA
G.
% of IL10, TGFβ co-expressing CD11b+ cells (In total lung cells)
0.010
0.008
0.006
0.004
0.002
0.000
*
PBS
C5aRA
H.
% of T-regs (In total lung cells)
0.005
0.004
0.003
0.002
0.001
0.000
*
PBS
C5aRA
I.
No. of T-regs/ml of blood
2.0x10^7
1.5x10^7
1.0x10^7
5.0x10^6
0
*
PBS
C5aRA

Figure 4

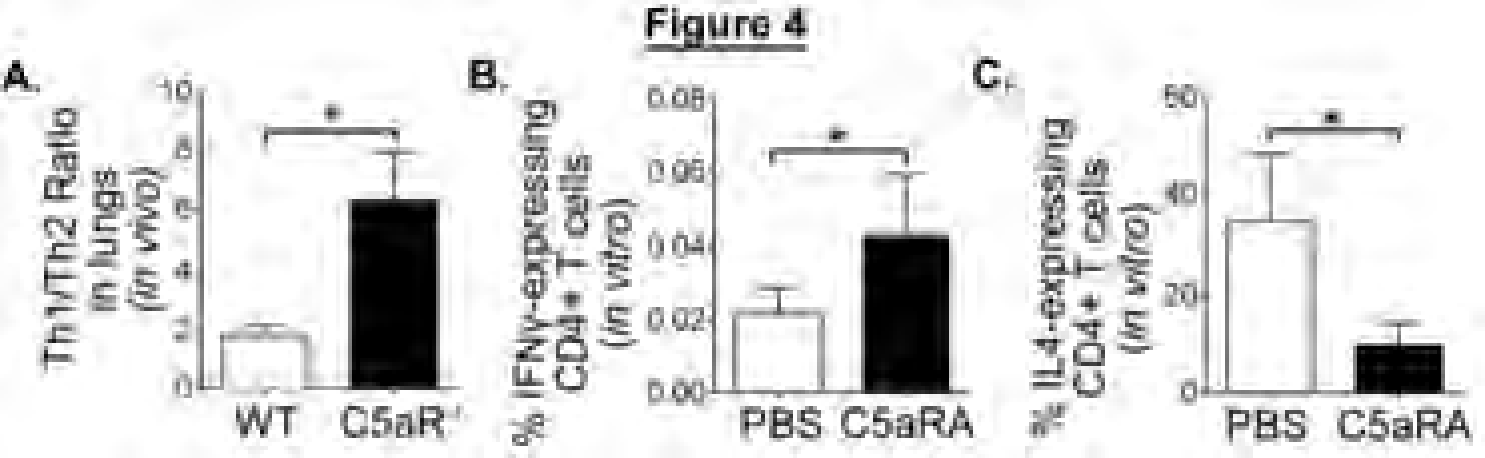
A.
Th1/Th2 Ratio in lungs (in vivo)
10
8
6
4
2
0
*
WT
C5aR-/-
B.
% IFNγ-expressing CD4+ T cells (in vitro)
0.08
0.06
0.04
0.02
0.00
*
PBS
C5aRA
C.
% IL4-expressing CD4+ T cells (in vitro)
60
40
20
0
*
PBS
C5aRA

Figure 5

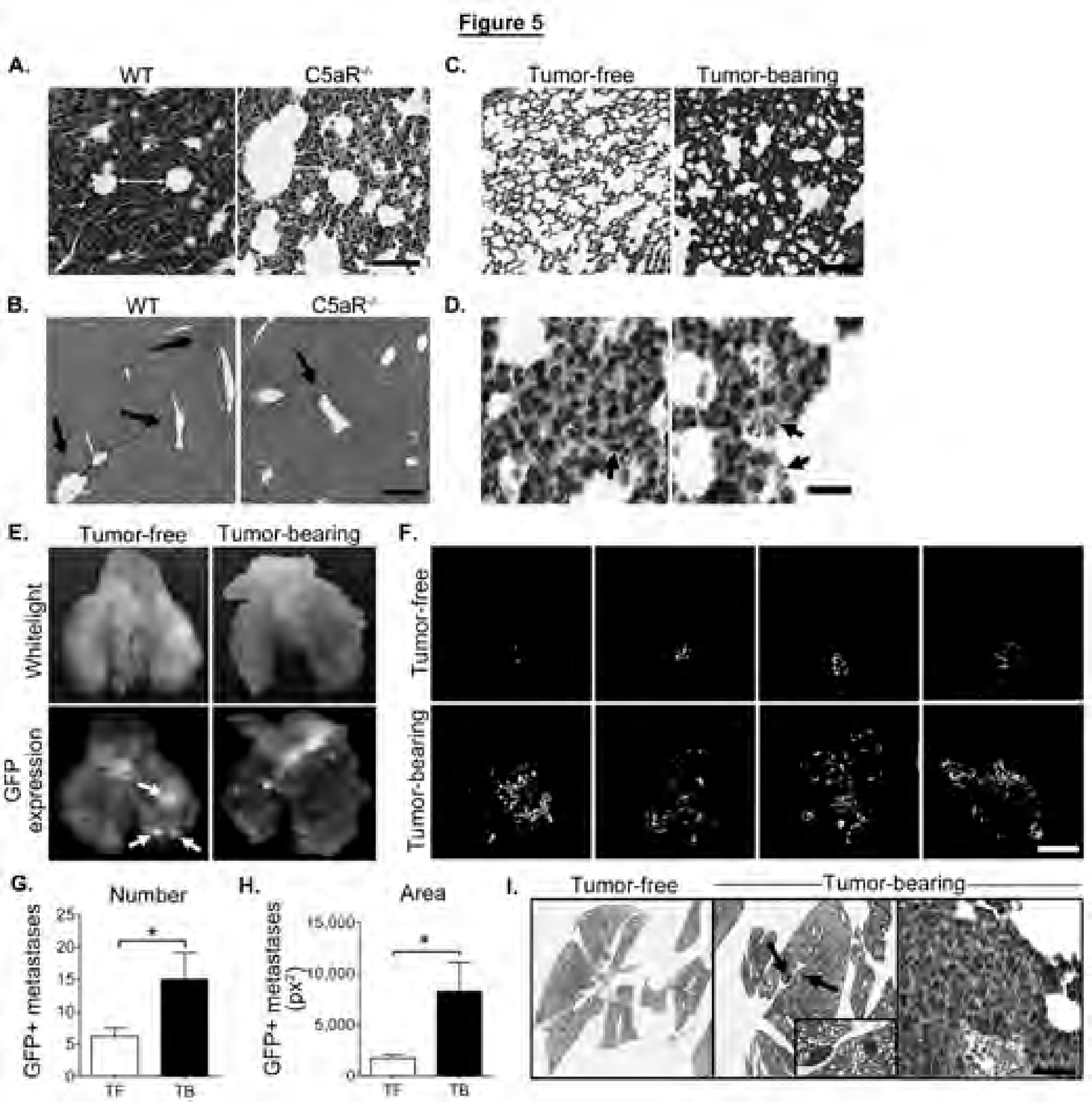
A.
WT
C5aR-/-
B.
WT
C5aR-/-
C.
Tumor-free
Tumor-bearing
D.
E.
Tumor-free
Tumor-bearing
Whitelight
GFP expression
F.
Tumor-free
Tumor-bearing
G.
Number
GFP+ metastases
25
20
15
10
5
0
TF
TB
H.
Area
GFP+ metastases (px²)
15,000
10,000
5,000
0
TF
TB
I.
Tumor-free
Tumor-bearing

Figure 6

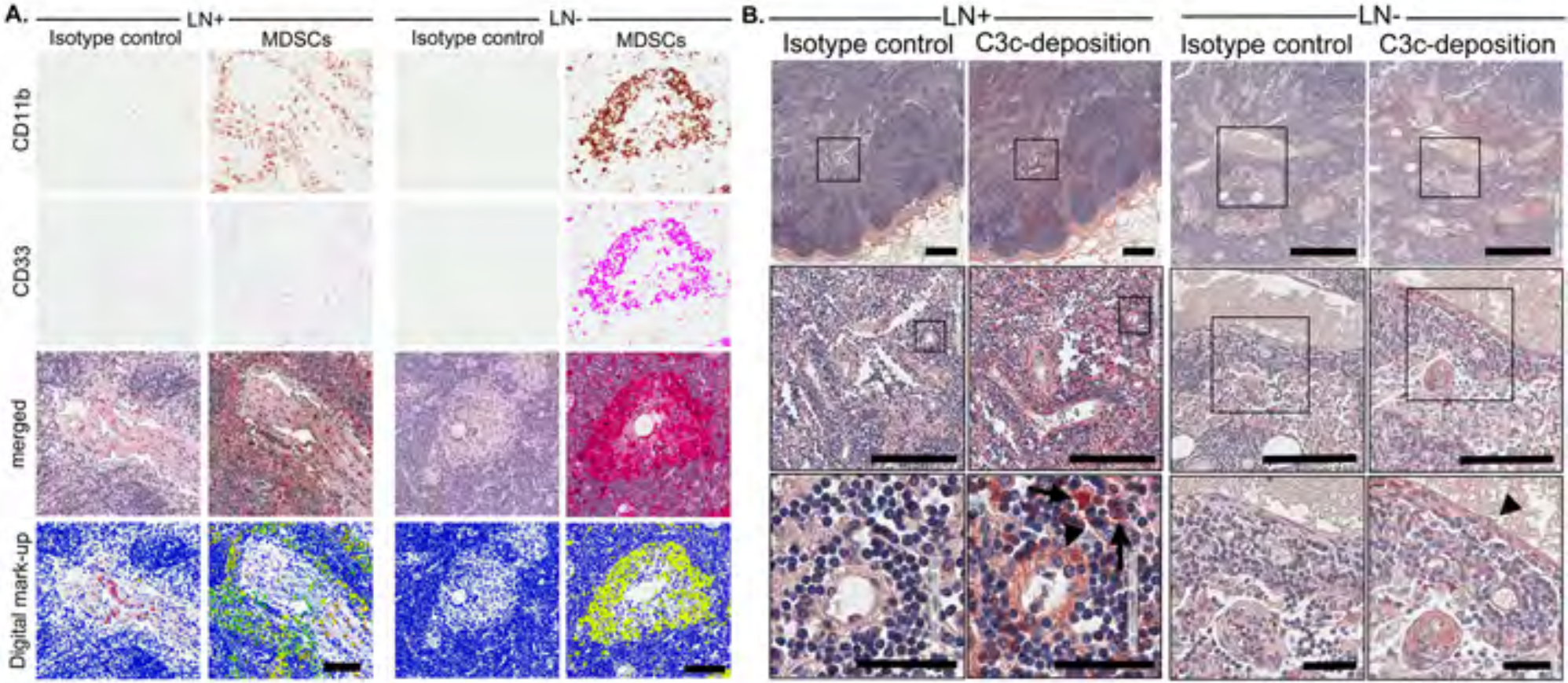
A.
LN+
Isotype control
MDSCs
LN-
Isotype control
MDSCs
CD11b
CD33
merged
Digital mark-up
B.
LN+
Isotype control
C3c-deposition
LN-
Isotype control
C3c-deposition